AUTOMATED GAUSSIAN FILTERING VIA GAUSSIAN SCALE SPACE AND LINEAR DIFFUSION

Eva Rifkah and Aishy Amer

Department of Electrical and Computer Engineering
Concordia University, Montréal, Québec, Canada
E-mail: e_erif,amer@ece.concordia.ca

ABSTRACT

Image denoising is challenging due to the difficulty to differentiate noise from image fine details. Convolution with a Gaussian mask is a widely used method for denoising. In this paper we propose, based on the relation between linear diffusion and Gaussian scale space, estimators of both the variance and window size of the discrete Gaussian filter applied to image denoising. To achieve content adaptive estimators, we also propose a structure under noise measure based on the median absolute deviation from the image gradient. Our simulations show that the proposed automated filter performs comparable or exceeds non-linear diffusion, while being of significantly lower complexity.

Index Terms— Denoising, Gaussian filter, Gaussian scale space, linear diffusion, variance, windows size.

1. INTRODUCTION

Noise is unavoidable signal added to real images and videos, even to those captured by modern high-end cameras. Denoising has been widely investigated but is still a challenging problem in real-world applications because of the high computational complexity of advanced denoising methods, and the difficulty to automatically differentiate noise from image fine detail. Gaussian filter is a well-known method for denoising but the adaptation of its parameters, the variance σ^2 and window size G, to the image content is a challenge. In this paper, based on the relation between Gaussian scale space (GSS) and linear diffusion (LD), we propose estimators for σ^2 and G towards an automated Gaussian filtering (AGSS).

Scale space is the concept to represent signals at different scales and is useful for several image processing applications. Convolving with a Gaussian function is a well-established solution to create a non-trivial linear scale space (LSS), that is causal, translation-invariant, and isotropic (e.g., [1, 2, 3]),

$$\begin{aligned} i(\mathbf{x};t) &= i(\mathbf{x};0) * g(\mathbf{x};t), \qquad t \geq 0 \\ &= \int_{\mathbb{R}^m} i(x_1 - a_1, \cdots, x_m - a_m; 0) \cdot g(\mathbf{a};t) d\mathbf{a}, \end{aligned} \tag{1}$$

where $*$ is the convolution operation, $i : \mathbb{R}^m \rightarrow \mathbb{R}$ is an m-dimensional continuous signal, $\mathbf{x} = \{x_1, x_2, \cdots, x_m\} \in \mathbb{R}^m$ is a location in the signal, $m \in \mathbb{N}$, $i(\mathbf{x};0)$ is the original input signal, $i(\mathbf{x};t)$ is the signal at scale t, and $\mathbf{a} = \{a_1, \cdots, a_m\}$. At scale t, the Gaussian function $g(\mathbf{x};t)$ is defined as,

$$g(\mathbf{x};t) = \frac{1}{(4\pi t)^{\frac{m}{2}}} e^{-\frac{x_1^2 + x_2^2 + \cdots + x_m^2}{4t}}. \tag{2}$$

$g(\mathbf{x};t) \geq 0$ is rotationally symmetric and separable. The Gaussian variance σ^2 that controls the information to be smoothed in the GSS is defined as,

$$\sigma^2 = t/2. \tag{3}$$

In discrete space $\mathbf{s}$ but still with continuous scale t, (1) becomes

$$i(\mathbf{s};t) = i(\mathbf{s};0) * g(\mathbf{s};t), \quad t \geq 0, \tag{4}$$

$i : \mathbb{Z}^m \rightarrow \mathbb{R}$ and $\mathbf{s} = \{s_1, s_2, \cdots, s_m\} \in \mathbb{Z}$.

Convolution with Gaussian in (1) is the solution to the *heat equation*,

$$\frac{\partial}{\partial t} i(\mathbf{x};t) = C \cdot \Delta i(\mathbf{x};t), \tag{5}$$

where Δ is the continuous Laplacian operator, defined as the divergence of the signal gradient ∇i, C is a constant. With the initial condition $\lim_{t \rightarrow 0} i(\mathbf{x};t) = i(\mathbf{x};0)$ and imposing the linearity and causality properties. The discrete heat equation from (5) can be written as,

$$\frac{\partial}{\partial t} i(s;t) = i(s;t) * a_L, \tag{6}$$

where a_L is a multiple of the discrete Laplacian operator [2].

Equation (6) is discrete in space s, but continuous in scale t. To solve this partial differential equation with respect to t, one could approximate it via the Euler scheme, and the resulting discrete LD equation is,

$$i_s^{n+1} = i_s^n + \lambda \cdot \sum_{p \in W} \nabla i_p^n \tag{7}$$

with $|W|$ is the number of directions along which LD is computed, often $W = \{North, South, East, West\}$, s is the center pixel, $1 \leq n \leq N$ is the current scale, N is the number of iterations, $i_s^n = i(s,n)$ is the image intensity at s and n, i_s^{n+1} is the next scale of i^n, $\nabla i_p = (i_p - i_s)$ is the image gradient in direction p, and λ is the time step (or stability parameter) responsible for the stability of the difference equation (7), e.g., $\lambda = \frac{1}{4}$. The relation between t in (5) and n in (7) is

$$t = \lambda \cdot n. \tag{8}$$

In this paper, to achieve an adaptive estimation of the Gaussian filter, we first study the behavior of image structure under noise and propose a measure to estimate such structure. Then we relate the Gaussian variance to the LD stopping time and the Gaussian window size to that estimated variance and to the noise standard deviation. The rest of this paper is organized as follows. Section 2 proposes the structure under noise measure. Section 3 proposes our automated Gaussian filtering (AGSS). Section 4 presents simulation results. We conclude the paper in section 5.

2. ESTIMATING IMAGE STRUCTURE UNDER NOISE

The median absolute deviation of the image gradient (MAD) is a robust scale estimator [4, 5] that can be used to estimate the image global structure. However, considering noise, MAD does not accurately reflect the image noise-free structure. For low structure images, the MAD increases faster with noise than for high structure images. This is because the image structure hide the added noise (which is in accordance with the human perception of noise, i.e., the total perceived noisiness in an image decreases in high frequencies [6]). Table 1 compares the increase of MAD under noise (from the noise-free case to 20dB PSNR) for selected test images, see Fig. 5. Thus, to account for both noise and image structure,

	20dB	25dB	30dB	35dB	40dB	Org
MAD_{Gray}	24.41	13.70	7.69	4.29	2.37	0.00
$\text{MAD}_{\text{Peppers}}$	25.63	15.06	9.20	6.09	4.52	3.00
$\text{MAD}_{\text{Baboon}}$	29.90	20.93	15.95	13.17	12.18	11.50
$\text{MAD}_{\text{Peacock}}$	33.44	25.28	21.21	19.60	19.09	19.00

Table 1: Comparing MAD of increasingly structured images under noise. 'Org' is the "noise-free" image.

we propose a structure-under-noise estimator ρ as the ratio between the estimated noise standard deviation and the MAD,

$$\begin{aligned} &\rho = \frac{\eta}{\text{MAD}}, \\ &\text{MAD} = \text{median}(\| \nabla I - \text{median}(\| \nabla I \|) \|). \end{aligned} \tag{9}$$

where η^2 is the noise variance. Fig. 1 shows how the proposed structure-under-noise estimator well distinguishes between the selected test images under different noise η. Small ρ means higher structure than noise. High ρ means the noise dominates (i.e., more visible) the image structure. For example, in *Gray* image, $\rho \simeq 1$ for all noise levels because, the image has no structure.

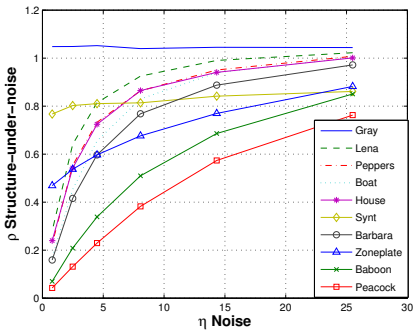

Figure 1: $\rho = \eta/\text{MAD}$ as a function of the input noise.

3. AUTOMATED GAUSSIAN FILTERING AGSS

In this section, we estimate the variance σ^2 and window size G of the Gaussian function via estimating N and λ of LD. For this, we study the relation between N, λ, and η. For a noise level η, the higher N is, the smaller the needed λ is (see Fig. 2a). Fig. 2b confirms, the proportion between N and λ for an optimal denoising. We conclude that for a fixed noise level η, N and λ are inverse proportional.

Noise is undesirable structure and thus to moderate the proportion between noise and λ we study the relation between λ and ρ. Fig. 3 shows that λ is proportional to ρ, i.e., the higher ρ is the bigger λ should be. In the case when $\rho \to 1$, the image is either of low structure or very high noise. In both cases we need bigger λ to perform effective denoising.

Now, we fix λ and study what N is optimal to achieve highest PSNR gain for different noise levels. Fig. 4 displays the proportion between N and noise for a fixed $\lambda = 0.1$ for Lena, an image with medium structure: the higher the noise is, the more N is required but a very high N will cause the PSNR gain to drop. In fact we notice that for any input noise level, there is a minimum N required to achieve a reasonable PSNR. Now, for images such as Baboon, such minimal or maximal N must be different so to preserve the image structure. Thus we not only need to consider noise but structure under noise, represented by the proposed ρ in (9).

Following the above findings, we propose the following λ and N estimators:

$$\lambda = \rho \cdot \lambda_{max}, \tag{10}$$

where $\lambda_{max} = \frac{1}{4}$ assuming 4-neighborhood (see [7] and [8]).

$$N = \rho \cdot \sqrt{\eta}. \tag{11}$$

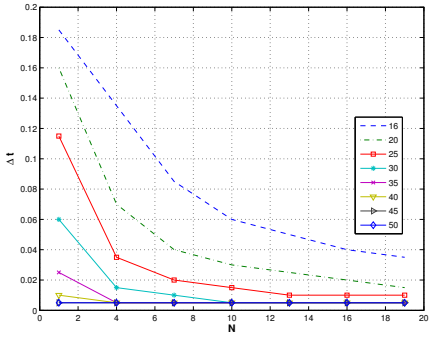

(a) λ versus N for different noise levels; Barbara.

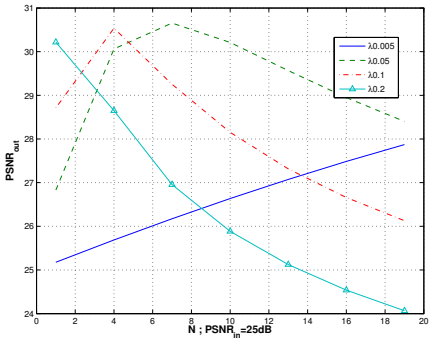

(b) N versus λ for 25dB; Lena.

Figure 2: Dependencies between N, λ, η.

Now to estimate the Gaussian filter parameters, we relate LD and GSS as follows. We know that $\sigma^2 = 2t$ and with (8), (10) and (11), our estimator for σ^2 is,

$$\sigma^2 = \rho^2 \cdot 2 \cdot \lambda_{max} \cdot \sqrt{\eta} \tag{12}$$

Our adaptive estimator for G of the Gaussian function is,

$$G = \sqrt{\eta_{max}} \cdot \sigma, \tag{13}$$

where η_{max} is the maximum possible noise standard deviation, e.g., equivalent to 10dB. We see that G is adaptive to the Gaussian variance proportional to the maximum assumed noise. With relating σ and G, the filter decays to nearly zero at edges, and we will get no discontinuities in the filtered image. In implementations, we round G to the nearest odd integer.

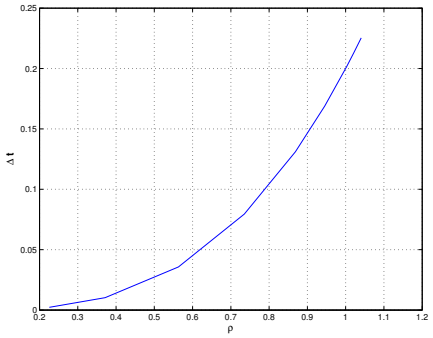

Figure 3: Relation between λ and ρ; Peppers.

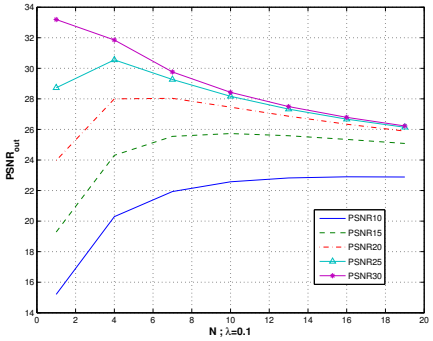

Figure 4: N versus the added noise for certain λ; Lena.

Figure 5: Test images used: Gray, Zoneplate, Synt, House, Peppers, Lena, Boat, Barbara, Baboon, Peacock.

4. SIMULATION RESULTS

We compare our AGSS with the non-linear diffusion method of Weickert [9]. This method estimate the stopping time of Perona and Malik [10] anisotropic diffusion (AD) model,

$$i_s^{n+1} = i_s^n + \lambda \sum_{p \in W} C(\nabla i_p^n, \sigma_{AD}) \cdot \nabla i_p^n, \tag{14}$$

where $C(\nabla I_p, \sigma)$ is the edge-stopping function in direction p and σ_{AD} is the edge strength to control the shape of $C(\cdot)$. This method works well for images of high structure, but has high computational cost.

As can be seen in Fig. 6, AGSS removes noise while preserving the image structure without introducing blurring for either low and high noise. Objectively, Table 2 gives average gain in the PSNR sense, over eight images, using our AGSS, with estimated parameters G and σ^2. As can be seen, AGSS achieves high PSNR for the different images, despite being linear in nature. This is because, with the automated Gaussian filter, practically we are estimating the required time for the denoising process as well as controlling σ^2 and the filter size. Thus, we avoid blurring the image. We see in Table 2 how well adapted the size and variance to the input noise.

Fig. 7 compares the performance of the proposed AGSS with the non-linear diffusion of Weickert. As can be seen,

(a) Denoising under 25dB. (b) Denoising under 40dB.

Figure 6: Denoising using AGSS for different noise; Boat

$PSNR_{in}$	11	15	20	25	30	35	40
Size G	9	8	6	6	4	3	2
Variance σ^2	1.03	0.90	0.74	0.59	0.44	0.30	0.19
$PSNR_{AGSS}$	20.3	23.1	25.8	28.7	31.9	35.5	40.0

Table 2: Estimated parameters and average output PSNR for AGSS over *Peppers, Lena, Field, House, Boat, Barbara, Baboon* and *Peacock*.

AGSS has comparable results under high noise, and outperforms non-linear diffusion under low noise. The computational cost of AGSS is much less than non-linear diffusion.

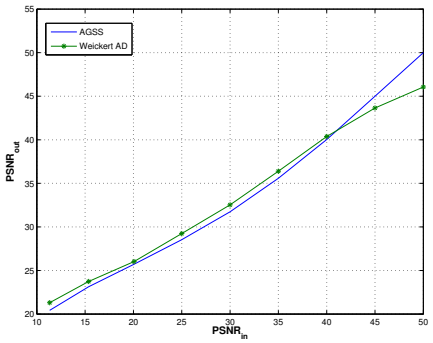

(a) PSNR comparison.

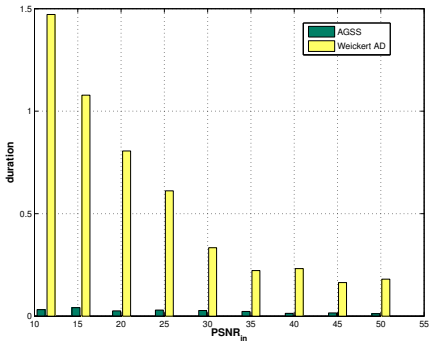

(b) Computational cost (in seconds) comparison.

Figure 7: Comparing proposed AGSS to non-linear diffusion, averaged over the images *Lena*, *Barbara*, and *Baboon*.

5. CONCLUSION

In this paper, we revisited Gaussian filter for image denoising, where we studied the relation between Gaussian scale space and linear diffusion and derived estimates for the Gaussian variance and window size. To adapt the estimates to image structure, we proposed a structure measure using the the noise variance and the median absolute deviation of the image gradient. Simulations show that the proposed estimators well adapt the Gaussian convolution to images of different structure and noise levels for effective fast denoising. The proposed method gave similar or better results compared to non-linear diffusion filters, with much less computational cost.

6. REFERENCES

[1] J.J. Koenderink, "The structure of images," *Biological Cybernetics*, vol. 50, pp. 363–370, 1984.

[2] T. Lindeberg, "Scale-space for discrete signals," *IEEE Trans. Pattern Anal. Mach. Intell.*, vol. 12, no. 3, 1990.

[3] A. Cunha, R. Teixeira, and L. Velho, "Discrete scale spaces via heat equation," in *Brazilian Symposium on Computer Graphics and Image Processing*. 2001, pp. 68–75, IEEE Computer Society.

[4] F. Mosteller and J. Tukey, *Data Analysis and Regression*, Addison-Wesley, 1977.

[5] Z.Y Zhang, "Parameter estimation techniques: a tutorial with application to conic fitting," *Image and Vision Computing*, vol. 15, pp. 59–76, 1997.

[6] T. Fujio, "A universal weighted power function of television noise and its application to high-definition TV-system design," *IEEE Trans. Broadc.*, vol. BC-26, no. 2, pp. 39–48, 1980.

[7] G. Gerig, O. Kubler, R. Kikinis, and F.A. Jolesz, "Nonlinear anisotropic filtering of MRI data," *IEEE Transactions on Medical Imaging*, vol. 11, no. 2, pp. 221–232, 1992.

[8] Joachim Weickert, Bart M. Ter Haar Romeny, and Max A. Viergever, "Efficient and reliable schemes for nonlinear diffusion filtering," *IEEE Trans. Image Process.*, vol. 7, no. 3, pp. 398–410, 1998.

[9] J. Weickert, "Coherence-enhancing diffusion of colour images," *IVC*, vol. 17, no. 3/4, pp. 201–212, March 1999.

[10] P. Perona and J. Malik, "Scale-space and edge detection using anisotropic diffusion," *IEEE Trans. Pattern Anal. Machine Intell.*, vol. 12, no. 7, pp. 692–639, 1990.